Mutual Synchronization of Molecular Turnover Cycles in Allosteric Enzymes. II. Product Inhibition

ARTICLE *in* THE JOURNAL OF PHYSICAL CHEMISTRY B · JULY 1999

Impact Factor: 3.3 · DOI: 10.1021/jp9900640 · Source: OAI

3 AUTHORS, INCLUDING:

Alexander S. Mikhailov
Fritz Haber Institute of the Max Planck Society
285 PUBLICATIONS **6,220** CITATIONS

Mutual Synchronization of Molecular Turnover Cycles in Allosteric Enzymes II. Product Inhibition

P. Stange,[†] A. S. Mikhailov,* and B. Hess[‡,§]

Fritz-Haber-Institut der Max-Planck-Gesellschaft, Faradayweg 4−6, D-14195 Berlin, Germany, and Max-Planck-Institut für molekulare Physiologie, Otto-Hahn-Str. 11 D-44227 Dortmund, Germany[2]

Received: January 5, 1999; In Final Form: May 11, 1999

Diffusion of regulatory molecules during an enzymic reaction in micrometer and submicrometer reaction volumes can lead to mixing and transport times much shorter than the turnover time of enzymes. Our theoretical investigations of a stochastic model of an allosterically product-inhibited enzymic reaction show that under these conditions the turnover cycles of individual enzymes can become synchronized. Interactions between different enzymes realized by means of fast moving inhibitor molecules are responsible for such mutual synchronization. This synchronization is accompanied by rapid oscillations in the concentration of the reaction product.

1. Introduction

Structural flexibility and conformational changes are essential for the biological function of enzymes.[1,2] Recent progress in time-resolved X-ray spectroscopy of protein crystals makes it already possible to investigate intramolecular processes and conformational changes in such macromolecules.[3−6] Single-molecule fluorescence spectroscopy opens the possibility to directly observe individual reaction events on the molecular level.[7−12] Furthermore, new experimental methods already allow to investigate complete enzymic reactions in biologically relevant nanoenvironments.[13]

Additional information is provided by current theoretical research on the statistical physics of heteropolymers.[14−17] These studies indicate that conformational relaxation in proteins can be a slow kinetic process taking milliseconds or longer, because such macromolecules resemble spin glasses and have a large number of quasi-equilibrium states corresponding to local minima of free energy.

It was found in the experiments with the photosensitive cytochrome P-450 dependent monooxygenase system[18−20] that the turnover cycles of individual enzymes could be synchronized by applying periodic light flashes. Another type of external synchronization has been discussed in the membrane transport system of the enzyme Na,K-ATPase using external electric fields (see, e.g., ref 21). Using a simple model, we have recently shown that mutual synchronization of individual turnover cycles of enzymes can take place in reactions with allosteric product activation.[22−24] This synchronization does not require any external forcing and represents an effect of microscopic self-organization in such a nonequilibrium system. The aim of this paper is to show that similar effects can also be observed in enzymic reactions with product inhibition. In contrast to the externally induced effect, mutual synchronization can develop only inside sufficiently small reaction volumes where diffusional mixing and transport times of substrate and products are much shorter than the turnover time of a single catalytic cycle.[25,26] For millisecond turnover times these conditions are satisfied in micrometer and submicrometer volumes, containing only hundreds or thousands of enzymes.

Under such conditions the situation differs from that described in macroscopic reaction kinetics, because the physics of the intramolecular processes in single enzyme molecules depends on conformational relaxation being much slower than the kinetic diffusion-related processes. Therefore, the population of such macromolecules can form a highly correlated "molecular network" where coherent collective behavior is possible. Our previous studies have shown that such coherent behavior can persist even when fluctuations in the duration of individual cycles are relatively intensive.[24]

In this paper we consider theoretically an example of a hypothetical product-inhibited enzymic reaction and show that the phenomena of mutual synchronization of molecular turnover cycles are also possible for such reactions, though they have certain features that make them different from the respective behavior previously discussed by us for the product-activated allosteric enzymic reactions.[24] In the next section we introduce a stochastic model of the considered reaction. The results of numerical simulations of this model are presented in section 3. The mean-field approximation is constructed in section 4 and used to analytically determine the synchronization boundaries in the parameter space. Two modifications of the stochastic model, involving different assumptions about the binding mechanism of inhibitory molecules, are investigated in section 5. We summarize the results of our theoretical study in the final section. The Appendix presents the algorithm used in our numerical simulations of the stochastic model.

2. Stochastic Model of a Product-Inhibited Enzyme Reaction

To investigate mutual synchronization of catalytic cycles of product-inhibited allosteric enzymes, we choose a hypothetical single substrate reaction where binding of a substrate molecule initiates the catalytic turnover cycle leading to the release of a product molecule. In our simple model we assume that the product molecules play a regulatory role and allosterically inhibit binding of the substrate molecules to the same enzyme. A free

* Corresponding author. E-mail: mikhailov@fhi-berlin.mpg.de.
[†] Fritz-Haber-Institut der Max-Planck-Gesellschaft.
[‡] Max-Planck-Institut für molekulare Physiologie.
[§] Current address: Max-Planck-Institut für medizinische Forschung, Jahnstrasse 29, D-69120 Heidelberg, Germany.

10.1021/jp9900640 CCC: $18.00
Published on Web 07/02/1999

product molecule can bind to the enzyme at a specific site which is spatially separated from that of the substrate molecule. Dissociation of the product molecule from the regulatory site recovers the enzyme activity. Product molecules decay or are removed at a certain rate from the reaction volume by other chemical reactions.

We assume that this reaction proceeds in a small volume, so that the conditions of a molecular network are satisfied. These conditions are[22,26,27]

$$\tau \gg t_{\text{transit}} > t_{\text{mix}} \tag{1}$$

Here τ is the turnover time, i.e., the time needed by an enzyme molecule to transform the substrate molecule into the product and return to its initial state where it can again bind a substrate molecule; t_{mix} is the diffusive mixing time of product molecules in the reaction volume, and t_{transit} is the transit time needed by a product molecule to reach by diffusion an enzyme and bind at the regulatory site on its surface. If $t_{\text{transit}} > t_{\text{mix}}$, the initial position of a product molecule is already forgotten when it binds to an enzyme and therefore it can bind with the same probability to any enzyme molecule in the reaction volume. This means that the system is perfectly mixed and the spatial coordinates of molecules are irrelevant. The condition $\tau \gg t_{\text{transit}}$ implies that the transport time of messenger molecules (products) is much shorter than the duration of a single molecular catalytic cycle. In this case the reacting system can be viewed as a population of fast communicating dynamical elements with slow cyclic dynamics.

The characteristic mixing and transit times for the regulatory molecules in a reaction volume of linear size L containing N enzymes are given, respectively, by the estimates $t_{\text{mix}} = L^2/D$ and $t_{\text{transit}} = L^3/NDR$ where R is the radius of the atomic target group on the surface of the enzyme molecule, representing its regulatory binding site, and D is the diffusion constant of regulatory molecules. Therefore the condition $t_{\text{transit}} > t_{\text{mix}}$ implies that the total number of enzyme molecules in the reaction volume is smaller than $N_{cr} = L/R$. For a micrometer reaction volume and a target group of a nanometer radius, this yields $N_{cr} = 1000$ which is about 10^{-6}M.[26]

In molecular networks the dynamical properties of each single enzyme are important. The actual intramolecular dynamics of such macromolecules is extremely complex and only globally known. To model these intramolecular processes large simplifications are needed. Following our previous publications[23,24] (see also ref 22), the dynamics of a single enzyme molecule during the catalytic turnover cycle is modeled below as diffusive motion along a given reaction coordinate. The enzymic cycle includes also such stochastic events as binding and dissociation of substrate and regulatory molecules (Figure 1).

It is convenient to define for each enzyme i a binary variable s_i, such that $s_i = 0$, if the enzyme is in its free state ready to bind a substrate molecule. The formation of an enzyme−substrate complex is then described as a transition into the state with $s_i = 1$. This transition initiates the turnover cycle, which consists of the catalytic conversion of the substrate into the product and subsequent return of the enzyme to its free state. This process is modeled as diffusional drift through an energy landscape along the reaction coordinate ϕ_i. The coordinate $\phi_i = 0$ corresponds to the beginning of the cycle. The cycle ends when $\phi_i = 1$ and the enzyme returns to its free state with $s_i = 0$. The release of the product molecule takes place at point $\phi_i = \phi_c$ inside the cycle. Thus the point ϕ_c on the reaction coordinate separates two different processes. In the coordinate interval $0 < \phi_i < \phi_c$, the enzyme−substrate complex exists,

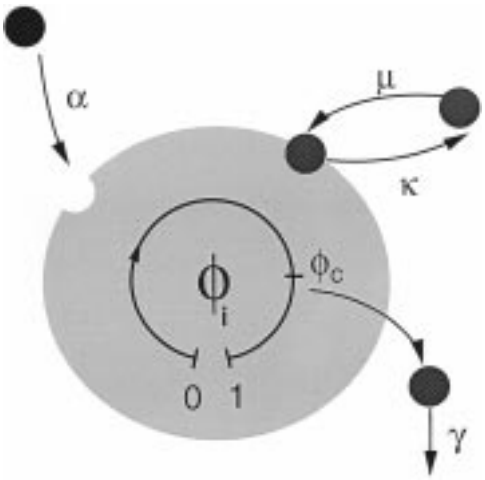

Figure 1. Schematic representation of an enzymic turnover cycle. The cycle is initiated by the binding of a substrate molecule at rate α and modeled as diffusive motion along the reaction coordinate ϕ increasing from $\phi = 0$ to $\phi = 1$. At stage $\phi = \phi_c$ inside the cycle, a product molecule is released that later decays at rate γ. Regulatory molecules can bind to the enzyme at rate μ and dissociate from it at rate κ. In our model, regulatory molecules are the product molecules of the same reaction.

whereas later in the interval $\phi_c < \phi_i < 1$ the enzyme returns back to its free state. There, it can again bind a substrate molecule to start a new cycle. Below we call ϕ the phase variable.

Introducing the probability distribution $p(\phi_i, t)$ over the coordinate ϕ_i, we assume that this distribution satisfies the diffusion equation

$$\frac{\partial p(\phi_i, t)}{\partial t} = -v\frac{\partial p(\phi_i, t)}{\partial \phi_i} + \sigma\frac{\partial^2 p(\phi_i, t)}{\partial \phi_i^2} \tag{2}$$

The first term in this equation describes the drift and the second term takes into account thermal fluctuations inside the cycle. The diffusion equation is equivalent to the following stochastic Langevin equation

$$\frac{d\phi_i}{dt} = v + \eta_i(t) \tag{3}$$

where v is the drift velocity, $\eta_i(t)$ is white Gaussian noise with the correlation function

$$\langle \eta_i(t)\eta_j(t')\rangle = 2\sigma\delta_{ij}\delta(t - t') \tag{4}$$

and the parameter σ determines the noise intensity. For simplicity, we assume in this model a constant negative slope of the energy landscape, so that the drift velocity v is constant. The drift velocity is used to define two characteristic times

$$\tau_1 = \frac{\phi_c}{v} \text{ and } \tau_0 = \frac{1}{v} \tag{5}$$

needed after cycle initiation, in the absence of fluctuations, to release a product molecule and to finish the cycle, respectively.

The cycle starts at $\phi = 0$ and ends after a certain time τ at $\phi = 1$. This is the turnover time that specifies the cycle duration. According to eq 3, the motion inside the cycle is a random process and therefore the turnover time fluctuates from one realization of this process to another. The mean turnover time is estimated as[24]

$$\langle\tau\rangle = \frac{1}{\upsilon} - \frac{\sigma}{\upsilon^2}[1 - \exp(-\upsilon/\sigma)] \quad (6)$$

and its statistical dispersion $\Delta\tau = \sqrt{\langle\tau^2\rangle - \langle\tau\rangle}$ is given by (see ref 24)

$$\Delta\tau^2 = \frac{2\sigma}{\upsilon^3} - \frac{5\sigma^2}{\upsilon^4} + \frac{4\sigma}{\upsilon^3}\exp(-\upsilon/\sigma) + \frac{4\sigma^2}{\upsilon^4}\exp(-\upsilon/\sigma) + \frac{\sigma^2}{\upsilon^4}\exp(-2\upsilon/\sigma) \quad (7)$$

The relative statistical dispersion is defined as

$$\xi = \frac{\Delta\tau}{\langle\tau\rangle} \quad (8)$$

For small noise intensities σ, the approximations $\langle\tau\rangle \approx 1/\upsilon$, $\Delta\tau \approx \sqrt{2\sigma/\upsilon^3}$, and $\xi \approx \sqrt{2\sigma/\upsilon}$ hold.

As said above, we consider the case where binding of the substrate is allosterically inhibited by product molecules. We assume that, in addition to the binding site for the substrate, the enzyme has another site where a regulatory molecule can bind. If the regulatory molecule is bound, the probability of binding a substrate molecule is strongly reduced. To describe this process we introduce for each enzyme i a second binary state variable r_i which is equal to 1, if the regulatory product molecule is bound to the regulatory site, and is otherwise zero. The probability α per unit time for an enzyme to bind a substrate molecule depends on r_i, i.e., $\alpha = \alpha_1$ if $r_i = 1$ and $\alpha = \alpha_0$ if $r_i = 0$. Note that in the considered case of inhibition $\alpha_0 \gg \alpha_1$. It is convenient to introduce the coefficient χ, characterizing the inhibition intensity and defined through $\alpha_1 = \alpha_0/\chi$. We assume that in our hypothetical reaction, the dissociation of the substrate is absent. The probability rate α is proportional to the substrate concentration. It is furthermore assumed that the substrate concentration is maintained constant.

The probability rate βm for binding a regulatory molecule, if m regulatory molecules are present inside the reaction volume, and the dissociation probability rate κ of regulatory molecules are both functions of s_i and ϕ_i. Different assumptions concerning these functions can be made. We first consider in the next section the model where the binding probability of regulatory molecules is equal to β, if $s_i = 0$, and is zero otherwise. In section 5 modifications of this model with other assumptions about these functions will also be considered. The dissociation probability rate κ is assumed to be constant independently on s_i and ϕ_i, if $r_i = 1$, and otherwise is zero.

The number m of free product molecules in the reaction volume is influenced by several processes. When an enzyme i reaches the point $\phi_i = \phi_1$ on the reaction coordinate, a product molecule is released. Moreover, each binding or dissociation event increases (decreases) this number m by one. To prevent accumulation of products, we assume that the product molecules decay at constant rate γ. The "decay" can actually represent the conversion of products that do not further participate in the reaction into other chemical species along a reaction pathway. Typically, we assume that the lifetime of free product molecules is short as compared with the turnover time, so that the condition $\gamma^{-1} \ll \tau$ holds.

The detailed algorithm used in numerical simulations of this stochastic model is described in the Appendix.

3. Coherent and Incoherent Enzyme Activities

In this section we present the results of our numerical investigations of the stochastic model. The total number of enzyme molecules is $N = 400$ in all simulations. We choose $\chi = 10^4$ and assume a drift velocity $\upsilon = 1$ in eq 3, and therefore $\tau_0 = 1/\upsilon = 1$. Unless specifically stated, the initial condition is always that all enzymes are randomly distributed over their cycle phases.

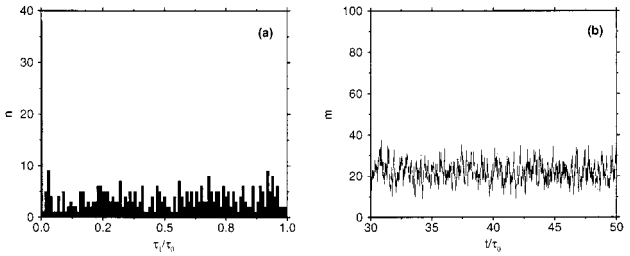

Figure 2. Distribution over cycle phases (a) and time dependence of the number of product molecules (b) for the asynchronous reaction regime in a population of $N = 400$ enzymes. The reaction parameters are $\beta = 0.03\tau_0^{-1}$, $\alpha_0 = 10\tau_0^{-1}$, $\chi = 10^4$, $\gamma = 15\tau_0^{-1}$, $\kappa = 20\tau_0^{-1}$, $\tau_1 = 0.55\tau_0$, $\upsilon = 1$, and $\sigma = 0$.

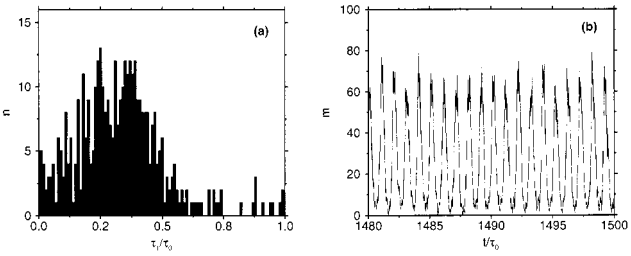

Figure 3. Distribution over cycle phases (a) and time dependence of the number of product molecules (b) for the synchronous reaction regime in a population of $N = 400$ enzymes. The reaction parameters are $\beta = 0.1\tau_0^{-1}$, $\alpha_0 = 100\tau_0^{-1}$, $\gamma = 15\tau_0^{-1}$, $\kappa = 20\tau_0^{-1}$, $\tau_1 = 0.55\tau_0$, $\upsilon = 1$, and $\sigma = 0$.

Simulations of the stochastic model show the existence of two qualitatively different regimes. Below a certain threshold of parameter β, which determines the probability rate for binding an inhibitory product molecule, the enzymes operate independently of each other. Figure 2a displays the distribution of enzymes over their phase variable ϕ in this case. To obtain this distribution, we determine the phases of all enzymes at a fixed time moment, divide the interval $0 \le \phi \le 1$ into 100 subintervals and count the number of enzymes in each of them. We see that the distribution is flat. This means that all phases are equally probable and there are no correlations between the internal states of different enzymes. The time dependence of the number of free product molecules in this case is shown in Figure 2b. Because of the incoherent enzyme activities, the number of products fluctuates around a certain mean value.

When the parameter β which characterizes the intensity of allosteric inhibition is increased, it is observed that the system behavior is drastically changed and the enzyme activity becomes coherent. Figure 3a shows a typical phase distribution of enzymes in the coherent regime. Now the distribution is not flat but contains a clear maximum. This means that correlations between different enzymes are present and their internal states are synchronized. Thus, almost all enzymes belong to a single coherent group. As shown in Figure 3b, the synchronous enzymic activity results in rapid periodic spiking in the number of free product molecules. The spiking period is determined by the turnover time of the enzymes. In our previous investigations of the product-activated enzyme reaction,[24] two or more groups of synchronized enzymes were found. In contrast to this, in the case of product inhibition only one coherent enzymic group is observed.

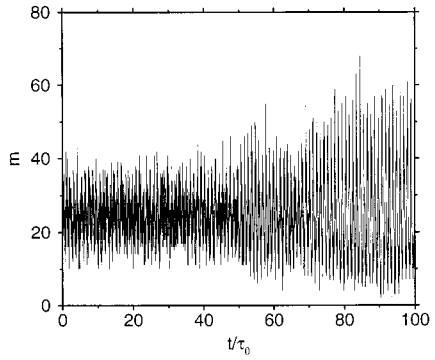

Figure 4. Transient behavior of the enzymic population starting from initial conditions with randomly distributed phases and leading to full synchronization of the entire population of $N = 400$. The reaction parameters are $\beta = 5\tau_0^{-1}$, $\alpha_0 = 100\tau_0^{-1}$, $\gamma = 15\tau_0^{-1}$, $\kappa = 20\tau_0^{-1}$, $\tau_1 = 0.55\tau_0$, $\upsilon = 1$, and $\sigma = 0.00125$.

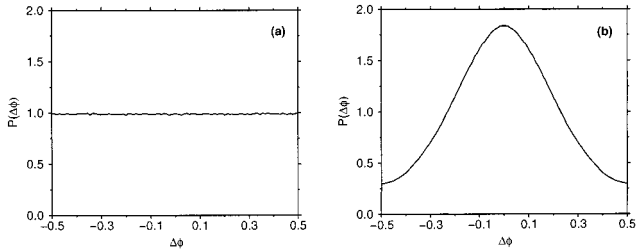

Figure 5. Distributions over phase differences in the typical kinetic regimes (a) without synchronization (parameters as in Figure 2) and (b) under synchronization of enzymic states (parameters as in Figure 3).

This transition to the coherent enzyme activity occurs spontaneously. At the initial moment $t = 0$ in our simulations, the enzymes are randomly distributed over their phases. But after a certain transient time, the states of enzymes become synchronized and spiking in the number product molecules is established (Figure 4). This transient time can strongly vary depending on β and the relative statistical dispersion ξ of the turnover time. For small values of ξ and β, as in Figure 3, the transient takes hundreds of turnover cycles. However, if the parameters ξ and β are larger, as in Figure 4, steady spiking of the products sets on already after a few turnover cycles.

To quantify the strength of synchronization, we introduce a special order parameter. Its definition is based on the distribution

$$P(\Delta\phi) = \langle [\sum_{i,j=1,i\neq j}^{N} s_i s_j]^{-1} \sum_{i,j=1,i\neq j}^{N} s_i s_j \delta(\phi_i - \phi_j - \Delta\phi) \rangle \quad (9)$$

that specifies the probability density to find a phase difference $\Delta\phi$ between two enzymes. Since $s_i = 0$ for enzymes in the free states, the summation is performed here only over enzymes inside their turnover cycles ($s_i = 1$). Angular brackets denote time averaging over sufficiently long intervals of time to eliminate fluctuations. The coefficient with square brackets in eq 9 represents the normalization factor; $\delta(x)$ is the Dirac delta function. When the phase states of different enzymes are not correlated, all phase differences are equally probable. Then the distribution $P(\Delta\phi)$ is flat (see Figure 5a). If however, the synchronization of enzymic states takes place, the probability distribution $P(\Delta\phi)$ shows a maximum at $\Delta\phi = 0$ (see Figure 5b).

The order parameter, characterizing the strength of synchronization, is defined as

$$\theta = \int_{-0.5}^{0.5} (P(\Delta\phi)^2 d\Delta\phi) \quad (10)$$

If the correlations between the phases of different enzymes are absent, $\theta = 0$. Nonvanishing values of θ indicate the presence of synchronization.

First, we study the influence of fluctuations inside the cycle on the synchronization phenomena by varying the noise intensity σ in our stochastic model while keeping fixed all other parameters. Figure 6a shows an example of the dependence of the order parameter θ on the relative statistical dispersion ξ of turnover time τ (see eq 8). With increasing ξ, the order parameter θ becomes smaller and is vanishingly small when ξ is larger than 0.1.

Next, we fix the noise intensity and increase the parameter β, characterizing the binding rate for the regulatory product molecules. Above a certain threshold the synchronization is found (see Figure 6b). Further increase of β increases the strength of the synchronization characterized by the order parameter θ. We find that there exists also an upper threshold for β above which the synchronization disappears. This means that only inside a certain window of β the synchronization is present. A similar result was already found in the case of product activation.[24]

In another series of simulations we calculate θ for different values of the parameter α_0, the binding probability rate for substrate molecules. As seen in Figure 6c a similar synchronization window is found also in the dependence on this parameter. In this case, the enzymic states do not synchronize below $\alpha_0 < 20\tau_0^{-1}$. In the interval $20 < \alpha_0 < 300$ the synchronization is present, whereas for higher values of α_0 it again disappears.

Finally, in Figure 6d the synchronization order parameter θ is plotted as function of κ, the dissociation rate of regulatory product molecules. The synchronization begins at approximately $\kappa \approx 4\tau_0^{-1}$, then the order parameter grows and reaches its maximum at $\kappa \approx 20\tau_0^{-1}$. At higher values of κ, the order parameter again decreases and the synchronization becomes weaker.

The typical time dependences of the number of products at different values of β are shown in Figure 7a−d. When the parameter β is small (Figure 7a, $\beta = 1.0\tau_0^{-1}$), spiking is absent. Above the synchronization threshold (Figure 7b, $\beta = 5\tau_0^{-1}$), spiking of products develops. The amplitude of spiking, however, decreases for higher values of β (Figure 7c, $\beta = 15\tau_0^{-1}$), and then spiking is already weak on the background of fluctuations (Figure 7d, $\beta = 20\tau_0^{-1}$).

Although simulations of the stochastic model given by eq 35−38 already provide much information about the behavior of the considered system, analytical studies are needed to predict the synchronization threshold and to better understand the synchronization phenomena. Such analytical investigations are reported in the next section.

4. The Mean-Field Approximation

The mean-field approximation in chemical kinetics consists of neglecting fluctuations in concentrations of reactants that are the result of the atomistic stochastic nature of reaction processes. In the limit $N \rightarrow \infty$ our system can be described by introducing two density functions $\tilde{n}_0(\phi, t)$ and $\tilde{n}_1(\phi, t)$, such that $\tilde{n}_0(\phi, t)\Delta\phi$ gives the mean number of enzymes, which have not bound a regulatory molecule and are found at time t inside the cycle in the phase states between ϕ and $\phi + \Delta\phi$, and $\tilde{n}_1(\phi, t)\Delta\phi$ represents the mean number of enzymes in the same interval which have bound a regulatory molecule. We also introduce the mean number $n_0(t)$ of enzymes, which are not inside the

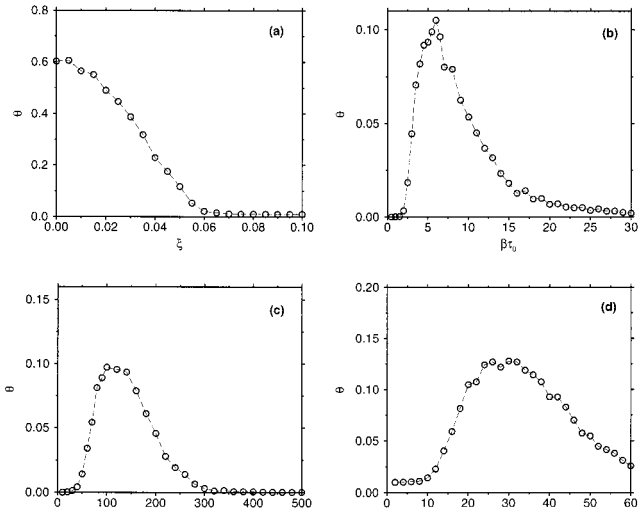

Figure 6. The order parameter θ as functions of (a) relative statistical dispersion ξ of the turnover time, (b) binding rate β for the regulatory molecules, (c) binding rate α_0 for the substrate molecules, and (d) dissociation rate κ for the regulatory molecules. When the parameters are fixed, they have the values $\sigma = 0.00125$ ($\xi = 0.05$), $\beta = 5\tau_0^{-1}$, $\alpha_0 = 100\tau_0^{-1}$, and $\kappa = 20\tau_0^{-1}$. Other parameters are $\gamma = 15\tau_0^{-1}$, $\tau_1 = 0.55\tau_0$, $v = 1$, and $N = 400$.

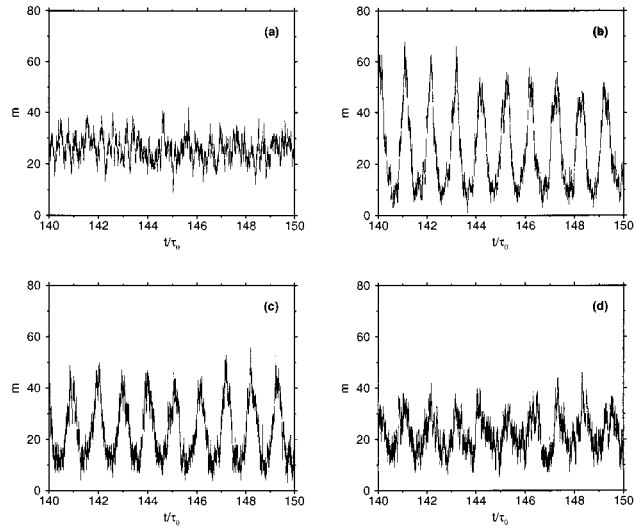

Figure 7. Time dependence of the number of product molecules for four different values of the binding rate for the regulatory molecules: (a) $\beta = \tau_0^{-1}$, (b) $\beta = 5\tau_0^{-1}$, (c) $\beta = 15\tau_0^{-1}$, and (d) $\beta = 20\tau_0^{-1}$. Other parameters are as in Figure 5.

cycle and have not bound a regulatory molecule, and the mean number $n_1(t)$ of enzymes, which are not inside the cycle but have bound a regulatory molecule. Moreover, $m(t)$ is the mean-number of product molecules at time t.

The mean-field evolution equations for $\tilde{n}_0(\phi, t)$ and $\tilde{n}_1(\phi, t)$ are

$$\frac{\partial \tilde{n}_1(\phi,t)}{\partial t} = -v\frac{\partial \tilde{n}_1(\phi,t)}{\partial \phi} - \kappa \tilde{n}_1(\phi,t) + \sigma\frac{\partial^2 \tilde{n}_1(\phi,t)}{\partial \phi^2} \quad (11)$$

and

$$\frac{\partial \tilde{n}_0(\phi,t)}{\partial t} = -v\frac{\partial \tilde{n}_0(\phi,t)}{\partial \phi} - \kappa \tilde{n}_1(\phi,t) + \sigma\frac{\partial^2 \tilde{n}_0(\phi,t)}{\partial \phi^2} \quad (12)$$

The evolution of the density functions $\tilde{n}_0(\phi, t)$ and $\tilde{n}_1(\phi, t)$ consists of the drift with constant velocity v accompanied by diffusion along the reaction coordinate ϕ. This diffusion is caused by intramolecular fluctuations with the intensity σ. Additionally, these equations take into account that the density $\tilde{n}_1(\phi, t)$ of inhibited enzymes inside the cycle decreases at rate κ because of the dissociation of regulatory molecules and that the density $\tilde{n}_0(\phi, t)$ increases because of this process. In the following analysis in this section we neglect intramolecular fluctuations inside the cycle by putting $\sigma = 0$ in eqs 11 and 12.

The boundary conditions for eqs 11 and 12 at $\phi = 0$ are

$$v\tilde{n}_1(\phi,t)|_{\phi=0} = \alpha_1 n_1(t) \quad (13)$$

$$v\tilde{n}_0(\phi,t)|_{\phi=0} = \alpha_0 n_0(t) \quad (14)$$

This means that free enzymes that bind substrate molecules and begin their cycles form incoming fluxes for the densities $\tilde{n}_1(\phi, t)$ and $n_0(\phi, t)$ at $\phi = 0$.

The evolution equation for the mean number of free inhibited enzymes has the form

$$\frac{dn_1}{dt} = \beta m(t) n_0(t) - \kappa n_1(t) - \alpha_1 n_1(t) + v\tilde{n}_1(\phi_0,t) \quad (15)$$

The first term on the right side of this equation takes into account that the number $n_1(t)$ of inhibited enzymes increases when free enzymes bind a regulatory molecule. The second term describes the dissociation of regulatory molecules from free enzymes. The third term takes into account the decrease in the number of free inhibited enzymes through binding of substrate molecules, and the last term describes the increase of $n_1(t)$ through enzymes finishing their cycles and returning to the free state. A similar equation holds for the number n_0 of free enzymes that have not bound a regulatory molecule:

$$\frac{dn_0}{dt} = -\beta m(t) n_0(t) + \kappa n_1(t) - \alpha_0 n_0(t) + v\tilde{n}_0(1,t) \quad (16)$$

Finally, the evolution equation for the mean number of product molecules in the reaction volume is

$$\frac{dm}{dt} = -\gamma m(t) + v\tilde{n}_1(\phi_c,t) + v\tilde{n}_0(\phi_c,t) + \kappa n_1(t)$$

$$-\beta m(t) n_0(t) + \kappa \int_0^1 \tilde{n}_1(\phi,t)d\phi \quad (17)$$

The first term on the right side describes the decay of product molecules. The second and the third terms take into account the release of new product molecules by enzymes at point $\phi = \phi_c$ inside the cycle. The fourth term corresponds to the increase in the number of products due to dissociation of regulatory molecules from free enzymes. The fifth term describes the decrease in the number of products by binding to free enzymes, and the last term takes into account dissociation of regulatory products from enzymes inside the cycle.

The total number

$$N = n_1(t) + n_0(t) + \int_0^1 \tilde{n}_1(\phi,t)d\phi + \int_0^1 \tilde{n}_0(\phi,t)d\phi \quad (18)$$

of enzymes in the system can be viewed as an integral of motion. This constant number N is equal to the sum of enzymes in the free state ($s = 0$) plus enzymes inside the catalytic cycle ($s = 1$ and $0 < \phi \leq 1$).

Equations 11−18 constitute the mean-field approximation. They can be reduced to a set of three differential delay equations. Note that eqs 11 and 12 can be solved for $\sigma = 0$ as

$$\tilde{n}_1(\phi,t) = \frac{\alpha_1}{\nu}\exp(-\kappa\phi/\nu)n_1\left(t - \frac{\phi}{\nu}\right) \quad (19)$$

$$\tilde{n}_0(\phi,t) = \frac{\alpha_1}{\nu}(1 - \exp(-\kappa\phi/\nu))n_1\left(t - \frac{\phi}{\nu}\right) + \frac{\alpha_0}{\nu}n_0\left(t - \frac{\phi}{\nu}\right) \quad (20)$$

Substituting the solutions for eqs 19 and 20 into eqs 16 and 17 and using the characteristic times defined by eq 5, we find the following set of evolution equations:

$$\frac{dn_1}{dt} = \beta m(t)n_0(t) - \kappa n_1(t) - \alpha_1 n_1(t) + \alpha_1 n_1(t-\tau_0)e^{-\kappa\tau_0} \quad (21)$$

$$\frac{dn_0}{dt} = -\beta m(t)n_0(t) + \kappa n_1(t) - \alpha_0 n_0(t) + \alpha_1 n_1(t-\tau_0)\,(1 - e^{-\kappa\tau_0}) + \alpha_0 n_0(t-\tau_0) \quad (22)$$

$$\frac{dm(t)}{dt} = -\gamma m(t) + \alpha_1 n_1(t-\tau_1) + \alpha_0 n_0(t-\tau_1) + \kappa n_1(t) - \beta m(t)n_0(t) + \kappa\int_0^{\tau 0}\alpha_1 n_1(t-t')e^{-\kappa t'}dt' \quad (23)$$

Below in this section we numerically integrate the mean-field equations 21−23 and compare their predictions with the behavior described by the original stochastic model. We also perform the linear stability analysis which allows us to derive the bifurcation diagram for this dynamical system and thus to analytically determine the synchronization thresholds.

Figure 8 displays the time dependence of the number of product molecules in the mean-field approximation. When the binding rate of regulatory molecules is low, spiking is absent and a transient leading to a constant level in the number of product molecules is observed (Figure 8a). For higher binding rates of regulatory molecules, persistent oscillations in the number of product molecules are observed (Figure 8b).

As noted above, fluctuations are neglected in the mean-field approximation, and it is therefore expected to hold only in the limit when the number of involved molecules goes to infinity. We have found, however, that even when the numbers of molecules are not very high and relatively strong fluctuations are present, the mean-field approximation still provides good estimates for the mean levels of product molecules as well as for the characteristic frequency and amplitude of the spikes.

The model parameters in Figures 2 and 3 are the same as in Figures 8a and 8b, respectively. Comparing Figures 2b and 8a, we find that the mean value of m in in the stochastic model in absence of synchronization (Figure 2b) coincides with the stationary level reached in Figure 8a. Under the synchronization conditions (Figure 3b and 8b), good agreement for the spiking regimes is furthermore found. This correspondence between the stochastic model and the mean-field approximation was observed in a wide range of parameters.

The boundaries of the spiking regimes in the parameter space are determined by the linear stability analysis. In absence of synchronization, in the mean-field approximation the system is found in the steady state corresponding to a fixed point. Analyzing the stability of this state with respect to small perturbations, the synchronization thresholds can be obtained.

First, we find the fixed point of eqs 21−23. To simplify the notations we perform the stability analysis choosing $\nu = 1$ which implies $\tau_0 = 1$. The total number N of enzymes is given by eq 18. If the system is found in the steady state $\bar{n}_0$, $\bar{n}_1$, and $\bar{m}$ eq

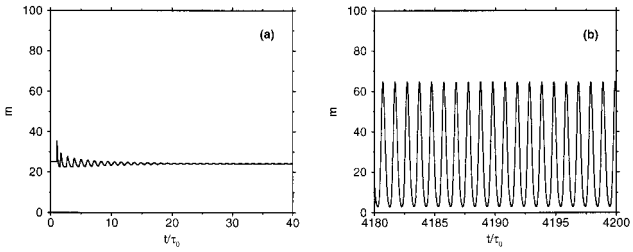

Figure 8. Time dependence of the number of product molecules obtained by integration of the mean-field equations (a) for the same parameters as in Figure 2, (b) for the same parameters as in Figure 3.

18 is simplified to

$$N = \bar{n}_1 + \bar{n}_0 + \alpha_1\bar{n}_1 + \alpha_0\bar{n}_0 \quad (24)$$

or

$$\bar{n}_0 = \frac{N - \bar{n}_1 - \alpha_1\bar{n}_1}{1 + \alpha_0} \quad (25)$$

Substituting this into eq 21 when $\dot{n}_1(t) = 0$ gives

$$\bar{n}_1 = \frac{\beta\bar{m}N}{\beta\bar{m}(1 + \alpha_1) + (\kappa + \alpha_1(1 - e^{-\kappa}))(1 + \alpha_0)} \quad (26)$$

Eliminating $\bar{n}_0$ and $\bar{n}_1$ in the stationary case in eq 23, we find

$$\bar{m}^2 + \bar{m}\frac{1}{1 + \alpha_1}\left[\frac{1}{\beta}(\kappa + \alpha_1\,(1 - e^{-\kappa}))(1 + \alpha_0) + \frac{N}{\gamma}(\kappa + \alpha_1(1 - e^{-\kappa})) - \frac{N}{\gamma}(\kappa + \alpha_1(2 - e^{-\kappa}))\right] - \frac{N\alpha_0(\kappa + \alpha_1(1 - e^{-\kappa}))}{\beta\gamma(1 + \alpha_1)} = 0 \quad (27)$$

This quadratic equation has two roots which can readily be calculated. Its solutions represent the number of product molecules in the steady state. Therefore, only the positive root of eq 27 is used. The solutions $\bar{m}$, $\bar{n}_0$, and $\bar{n}_1$ of equations 25−27 define the positive fixed point that corresponds to the steady state of the mean-field equations where phases are not correlated and the synchronization is absent.

Now the stability of this fixed point can be analyzed. Introducing small perturbations $m = \bar{m} + \delta m$, $n_0 = \bar{n}_0 + \delta n_0$, $n_1 = \bar{n}_1 + \delta n_1$, substituting them into eqs 21−23 and linearizing this system, we obtain

$$\frac{d\delta n_1}{dt} = \beta\bar{m}\delta n_0(t) + \beta\bar{n}_0\delta m(t) - \kappa\delta n_1(t) - \alpha_1\delta n_1(t) + \alpha_1\delta n_1(t-1)e^{-\kappa} \quad (28)$$

$$\frac{d\delta n_0}{dt} = -\beta\bar{m}\delta n_0(t) - \beta\bar{n}_0\delta m(t) + \kappa\delta n_1(t) - \alpha_0\delta n_0(t) + \alpha_1\delta n_1(t-1)(1 - e^{-\kappa}) + \alpha_0\delta n_0(t-1) \quad (29)$$

$$\frac{d\delta m}{dt} = -\gamma\delta m(t) + \alpha_1\delta n_1(t-\tau_1) + \alpha_0\delta n_0(t-\tau_1) + \kappa\delta n_1(t) - \beta\bar{m}\delta n_0(t) - \beta\bar{n}_0\delta m(t) + \kappa\int_0^1\alpha_1\delta n_1(t-t')e^{-\kappa t'}dt' \quad (30)$$

The solutions of these linear differential time-delay equations can be sought in the form $\delta n_1(t) = A \exp(\lambda t)$, $\delta n_0(t) = B \exp(\lambda t)$, and $\delta n_1(t) = C \exp(\lambda t)$. Substituting these solutions into eqs 28−30, we obtain a homogeneous system of linear equations

$$\hat{\mathbf{D}}\begin{pmatrix} A \\ B \\ C \end{pmatrix} = \lambda \begin{pmatrix} A \\ B \\ C \end{pmatrix} \tag{31}$$

with the coefficient matrix

$$\hat{\mathbf{D}} = \begin{pmatrix} \kappa + \alpha_1(a - e^{-\lambda-\kappa}) & \beta\bar{m} & -\beta\bar{n}_0 \\ -\kappa - \alpha_1 e^{-\lambda}(1 - e^{-\kappa}) & \beta\bar{m} + \alpha_0(1 - e^{-\lambda}) & \beta\bar{n}_0 \\ \dfrac{\alpha_1\kappa}{\lambda + \kappa}(e^{-\lambda-\kappa} - 1) - \kappa - \alpha_1 e^{-\lambda\tau_1} & \beta\bar{m} - \alpha_0 e^{-\lambda\tau_1} & \gamma + \beta\bar{n}_0 \end{pmatrix} \tag{32}$$

The solvability condition of this linear system is given by the characteristic equation

$$\det(\hat{\mathbf{D}} - \lambda\mathbf{I}) = 0 \tag{33}$$

This quasi-polynomial characteristic equation has an infinite number of complex roots $\lambda_j = \Gamma_j + i\omega_j$. If for a chosen set of parameters the real parts of all eigenvalues λ_j are $\Gamma_j < 0$, the steady state is stable. If for at least one eigenvalue $\Gamma_j > 0$, the steady state is unstable with respect to growth of oscillations with the frequency ω_j. The instability boundary is thus determined by the condition that $\Gamma_i = 0$ for at least one eigenmode j. Numerical investigations of eq 33 show that only for the lowest mode $j = 1$ with $\omega \approx 2\pi$ the real part Γ_i can become zero.

Figure 9a displays the bifurcation boundaries in the parameter plane (τ_1,β) obtained by numerical solution of eq 33 for two different substrate binding rates α_0. The steady state is unstable, and spiking develops inside closed regions bounded by the solid curves below and by dashed curves above. The large instability region in Figure 9a corresponds to the higher binding rate $\alpha_0 = 100\tau_0^{-1}$, whereas the smaller region corresponds to $\alpha_0 = 20\tau_0^{-1}$. Thus, if we keep τ_1 constant and increase the parameter β, the steady state becomes unstable and oscillations develop when the lower boundary (solid curves) is crossed. However, if we further increase β and cross the upper boundary (dashed curves), oscillations disappear and the steady state again becomes stable. This means that the synchronization is expected only in a certain window of the parameter β, in agreement with the results of our numerical simulations for the stochastic model (cf. Figure 6b). The synchronization window is more narrow (thin curve) when the substrate binding rate α_0 is decreased. Moreover, the synchronization is found only in a smaller interval of the parameter τ_1, i.e., only if the new product is released just slightly after the middle point of the cycle is passed.

The real part of λ vanishes on the bifurcation boundaries, whereas the imaginary part is finite. This imaginary part determines the frequency of oscillations that develop when the steady state loses its stability. In Figure 9b we plot the imaginary part of λ along the two bifurcation boundaries, shown in Figure 9a, as function of τ_1. The solid (dashed) curves in Figure 9b correspond to the parts of the bifurcation boundary in Figure 9a that are shown by the solid and dashed curves, respectively. We see that at the lower synchronization threshold for the higher value of the substrate binding rate α_0 the frequency of oscillations is close to $\omega_0/2\pi$, and therefore the temporal period is approximately equal to the molecular turnover time τ_0. Before the oscillations disappear at the upper boundary (dashed curve in Figure 9b), they have, however, a higher period. This is explained by stronger inhibition leading to the increase of the mean waiting times spent by free enzymes until they bind a substrate molecule.

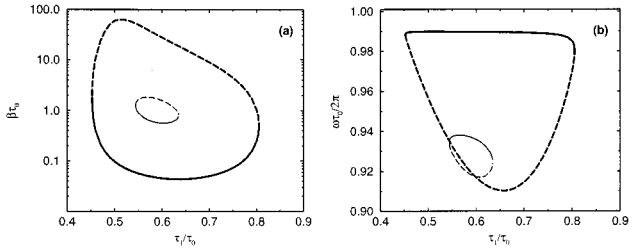

Figure 9. The bifurcation diagrams (a) in the parameter plane (τ_1/τ_0, $\beta\tau_0$) obtained by the stability analysis of the fixed point in the mean-field approximation for two different values of the substrate binding rate α_0. The thick curves are for $\alpha_0 = 100\tau_0^{-1}$ and the thin curves are for $\alpha_0 = 20\tau_0^{-1}$. The respective dependences (b) of the spiking frequencies on the bifurcation boundaries. Other parameters are $\gamma = 15\tau_0^{-1}$, $\kappa = 20\tau_0^{-1}$, and $N = 400$.

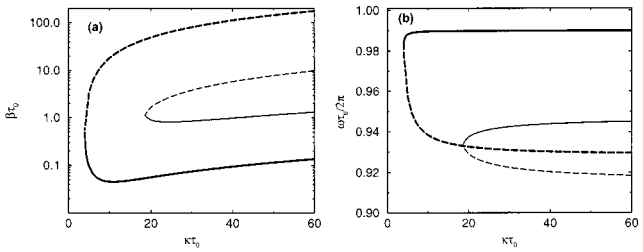

Figure 10. The bifurcation diagrams (a) in the parameter plane ($\kappa\tau_0$, $\beta\tau_0$) obtained by the stability analysis of the fixed point in the mean-field approximation for two different values of the substrate binding rate α_0. The thick curves are for $\alpha_0 = 100\tau_0^{-1}$ and the thin curves are for $\alpha_0 = 20\tau_0^{-1}$. The respective dependences (b) of the oscillation frequencies on the bifurcation boundaries. Other parameters are $\gamma = 15\tau_0^{-1}$, $\tau_1 = 0.55\tau_0$, and $N = 400$.

Figure 10a displays the bifurcation boundaries in the parameter plane (κ, β) for the same two substrate binding rates α_0 as in Figure 9. We use here the same notations as above. It is seen that the instability leading to spiking develops only when the dissociation rate κ exceeds a certain threshold depending on α_0 and β. Though the bifurcation boundaries are shown in Figure 10a only for $\kappa \leq 60$, we have numerically determined these boundaries also for much larger values of the dissociation rate of regulatory molecules. It was found that the synchronization window persists even when the dissociation rates are extremely high. This agrees with the numerical simulations of the stochastic model that show that the synchronization becomes weaker but does not completely disappear when κ is increased (cf. Figure 6d). Figure 10b shows the imaginary part along the bifurcation boundaries.

The numerical simulations of the nonlinear evolution eqs 21−23 of the mean-field approxmation show that, when the parameter β, characterizing the probability rate of enzymes to bind a regulatory molecule, is slowly increased, the stationary state indeed loses its stability at the point predicted by the bifurcation diagram. This leads to small oscillations, whose amplitude Δm has no jump at the instability point, i.e., the bifurcation is supercritical (Figure 11).

When the parameter β, characterizing the probability rate of enzymes to bind a regulatory molecule, is slowly increased, the numerical simulations show that the stationary state loses its

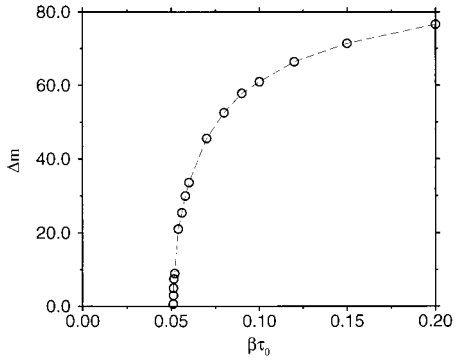

Figure 11. The oscillation amplitude Δm as function of the parameter β in the mean-field approximation for $\alpha_0 = 100\tau_0^{-1}$, $\gamma = 15$, $\tau_1 = 0.55\tau_0$, $\kappa = 20\tau_0^{-1}$, and $N = 400$.

stability at a point predicted by the bifurcation diagram. This leads to oscillations with a small amplitude Δm. We see in Figure 11 further that this amplitude grows continuously when β is increased, which is typical for a soft instability.

The dependence of the bifurcation boundaries on the total number N of enzymes in the reaction volume can easily be understood. Looking back at the mean-field eqs 11−18, we note that they are invariant under the scaling transformation $\beta \rightarrow$ b/c, $m \rightarrow cm$ and $n \rightarrow cn$ for any constant c. This transformation means simply that, if the total number N of enzymes is changed by a factor c, the numbers of product and substrate molecules in the volume are changed proportionally. The existence of this scaling transformation can be used to obtain the bifurcation boundaries for any N. For example, the bifurcation boundaries in Figure 9 are constructed for $N = 400$. If we want to find the bifurcation diagram for a larger system with $N = 4000$ enzymes, we must only replace β by β/10 in the original diagram. The same transformation should then be applied to the bifurcation diagram shown in Figure 10.

5 Two Modifications of the Inhibition Mechanism

In this section we investigate two modifications of the stochastic model with respect to binding of regulatory molecules by enzymes. In the stochastic model, numerically studied in section 3, binding of regulatory molecules by enzymes was only possible when an enzyme was in the free state, i.e., when the enzyme has finished its cycle but has not yet bound a substrate molecule. Generally, binding of a regulatory molecule may depend on the state of the enzyme. This dependence for real enzymes is not yet known and might be complicated. Below we consider two possible modifications and show, by numerical simulations, that the effect of mutual synchronization is present in both cases.

Modification 1. In the first modification of the original stochastic model it is assumed that an enzyme can bind a regulatory molecule with a constant probability rate in any of its states. This means that a regulatory molecule can also bind when the enzymes are inside their cycles. Thus, binding of a regulatory molecule by the enzyme i is now possible with the constant rate β independently of the enzymic state variables s_i and ϕ_i. As in the original model, dissociation of regulatory molecules does not depend on the enzymic state. Numerical simulations of this modified model were performed, and the results are presented below. In all of these simulations the total number of enzymes was $N = 400$, the drift velocity was $\upsilon = 1$, and the strength of inhibition characterized by χ was $\chi = 10^4$ as in section 3. To investigate the synchronization effect we again use the order parameter θ that was defined in eq 10. We

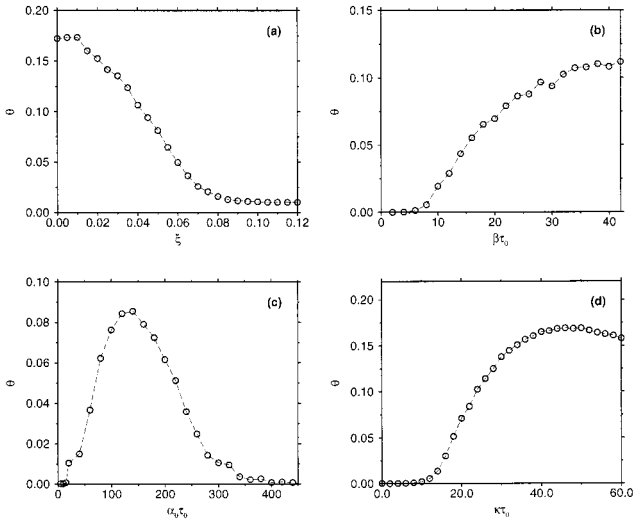

Figure 12. The order parameter θ as functions of (a) relative statistical dispersion ξ of the turnover time, (b) binding rate β for the regulatory molecules, (c) binding rate α_0 for the substrate molecules, and (d) dissociation rate κ for the regulatory molecules in modification 1. When the parameters are fixed, they have the values $\sigma = 0.00125$ ($\xi = 0.05$), $\beta = 20\tau_0^{-1}$, $\alpha_0 = 100\tau_0^{-1}$, and $\kappa = 20\tau_0^{-1}$. Other parameters are $\gamma = 25\tau_0^{-1}$, $\tau_1 = 0.55\tau_0$, $\upsilon = 1$, and $N = 400$.

wait until the transient is finished and then calculate θ, averaging over the time interval $4000\tau_0$ to eliminate random statistical variations. At first we study the influence of fluctuations inside the enzymic cycle. Keeping all other parameters fixed, the order parameter θ is calculated at different noise intensities σ (eqs 3 and 4) that determine according to eqs 6−8 the relative statistical dispersion ξ of turnover times. The result is displayed in Figure 12a. We see that the synchronization is present in the modified model. The dependence of θ on ξ is similar to that shown in Figure 6a. The synchronization persists up to the level $\xi \approx 0.1$.

Next, we fix the noise intensity and vary the parameter β characterizing the binding rate for the regulatory product molecules. Figure 12b shows the dependence of θ on β obtained by numerical simulations. Below $\beta = 5\tau_0^{-1}$ the synchronization is practically absent. The order parameter θ begins then to increase, and a monotonic growth is found even at very high binding rate constant β, in contrast to the original model where the synchronization was observed only inside an interval of β (Figure 6b).

In a different series of simulations, we vary the probability rate α_0 for binding a substrate molecule by the enzyme. The strength of synchronization θ as function of α_0 is shown in this case (Figure 12c). It turns out that at very low binding rates, $\alpha_0 < 30\tau_0^{-1}$, no synchronization is found. Inside the interval $30 < \alpha_0\tau_0^{-1} < 350$ the spiking exists, whereas at higher values of α_0 the synchronization again vanishes. Such a synchronization window in the dependence on the substrate binding rate was already found in Figure 6c. Finally, in Figure 12d the order parameter θ is plotted as function of κ, the dissociation rate of regulatory product molecules. The synchronization begins at $\kappa \approx 13\tau_0^{-1}$, then θ grows and saturates at $\kappa \approx 35\tau_0^{-1}$. This is different from the behavior found in the original model where a clear maximum was observed (Figure 6d).

Modification 2. In the second modification of the stochastic model, described in section 2, we assume that binding of regulatory molecules to an enzyme is possible with the same rate constant β in any of its states, except for the recovery period which begins after the release of the product molecule and ends when the enzyme returns to its free state. Thus, $\beta(s_i, \phi_i) = \beta$, if $s_i = 0$ or if $s_i = 1$ and $\phi_i < \phi_c$, and $\beta(s_i, \phi_i) = 0$ otherwise.

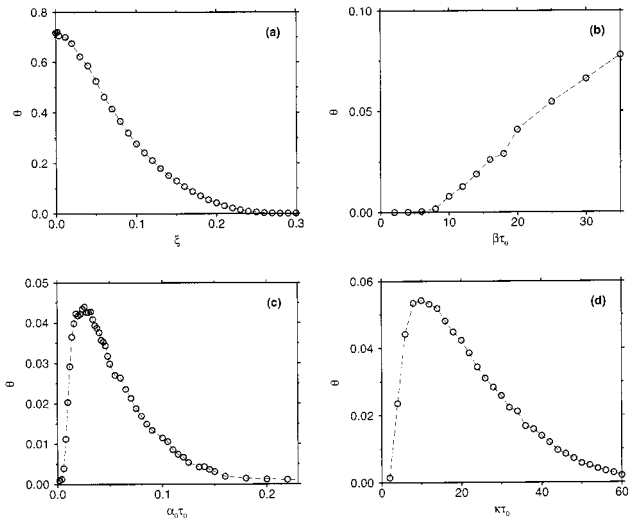

Figure 13. The order parameter θ as functions of (a) relative statistical dispersion ξ of the turnover time, (b) binding rate β for the regulatory molecules, (c) binding rate α_0 for the substrate molecules, and (d) dissociation rate κ for the regulatory molecules in modification 2. When the parameters are fixed, they have the values $\sigma = 0.03125$ ($\xi = 0.2$), $\beta = 20\tau_0^{-1}$, $\alpha_0 = 100\tau_0^{-1}$, and $\kappa = 20\tau_0^{-1}$. Other parameters are $\gamma = 25\tau_0^{-1}$, $\tau_1 = 0.55\tau_0$, $\upsilon = 1$, and $N = 400$.

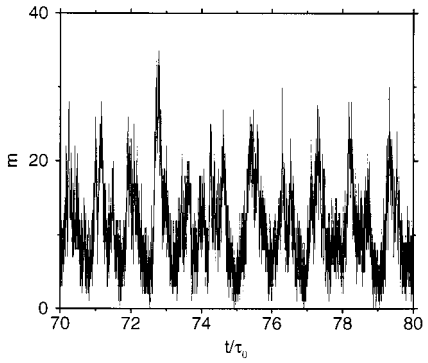

Figure 14. Spiking in the number of product molecules at a high noise intensity $\sigma = 0.08$ ($\xi = 0.4$) of intramolecular fluctuations in the model under modification 2. Other parameters are $\alpha_0 = 30\tau_0^{-1}$, $\beta = 30\tau_0^{-1}$, $\gamma = 25\tau_0^{-1}$, $\kappa = 20\tau_0^{-1}$, and $\tau_1 = 0.55\tau_0$, and $N = 400$.

Numerical simulations of this modified stochastic model are again performed with $N = 400$ enzymes and $\chi = 10^4$.

The results of our simulations show that the synchronization is also possible in this modified model and its properties are generally similar to what we have found before. However, the synchronization now persists up to much higher noise intensities corresponding to intramolecular dynamics. Figure 13a shows the computed dependence of the order parameter θ on the relative statistical dispersion ξ of turnover times in this case. We see that the synchronization order parameter θ vanishes only when the statistical dispersion is higher than $\xi = 0.3$. Remarkably, at other parameter values, spiking in the number of products is found in this modified model (Figure 14) even when the statistical dispersion of turnover times reaches ±40%! This means that such modification greatly increases the robustness of synchronization with respect to intramolecular fluctuations. Figures 13b, c, and d display the order parameter θ as functions of β, α_0, and κ. They are similar to the respective functions obtained in the first modified model. Note, however, that these dependences are now obtained for much higher intensity ($\xi = 0.2$) of intramolecular fluctuations.

6. Conclusions

In the previous publication[24] we considered simple models of product-activated allosteric reactions and found that these systems exhibit mutual synchronization of molecular turnover cycles. The action of allosteric inhibition is also widely observed in enzymic reactions. Our theoretical investigations in the present publication reveal that mutual synchronization of molecular cycles is equally possible for product-inhibited reactions. However, in this case the observed synchronization behavior shows a number of differences. Instead of the spontaneous formation of *several* coherent enzymic groups, characteristic for the product activation, in our present study we found that the intramolecular dynamics of the total molecular population tends to become synchronous at sufficiently strong product inhibition. This was observed in numerical simulations of the stochastic reaction model and was confirmed by the bifurcation analysis of the mean-field equations. Another interesting new aspect is that the synchronization was found now even at stronger intramolecular fluctuations, i.e., when the relative dispersion of turnover times reached ±40%.

We studied the synchronization phenomena under several different assumptions about the detailed mechanism of allosteric inhibition. The effect of allosteric inhibition in our model always consists of a decrease in the binding probability for substrate molecules when a regulatory molecule is bound at a separate site on the enzyme. However, the binding process of inhibitory molecules may have different properties. In the stochastic model formulated in section 2 we assumed that binding of inhibitory molecules was only possible if the enzyme had finished its turnover cycle. Alternatively, in section 5 we considered two model modifications where binding of inhibitory molecules was also possible for the enzymes during their turnover cycles. In the first modification an enzyme can bind an inhibitory molecule at any point inside its cycle, whereas in the second modification binding is not possible for enzymes that have released the product molecules and are returning to their free states. The synchronization behavior is found in all these cases and thus apparently represents a general property of product-inhibited enzymic reactions.

The dissociation of regulatory product molecules is possible, both inside the cycle and in the free state. Our numerical simulations and analytical investigations of the mean-field equations show however that a necessary condition for mutual synchronization is that the dissociation rate is so high that the mean time spent by a regulatory molecule, being bound to the enzyme, is shorter than the molecular cycle duration. Another necessary condition is that the mean lifetime of free product molecules in the reaction volume is also shorter than the cycle time.

Appendix

In this appendix we present the algorithm used in our numerical simulations of the stochastic reaction model, where time is divided in equal small steps Δt. The stochastic differential equation 3 corresponds to

$$\phi_i(t + \Delta t) = \phi_i(t) + \upsilon\Delta t + \varsigma_i\sqrt{\sigma\Delta t} \qquad (34)$$

where ς_i are independent Gaussian random numbers, such that

$$\langle\varsigma_i(t)\varsigma_j(t')\rangle = 2\delta_{ij}\delta(t - t')$$

Additionally, the dynamics of the phase variable at two special points should be defined. If at the next time moment $t + \Delta t$ the

phase $\phi_i(t + \Delta t)$ given by equation eq 34 is negative, we replace it by $\phi_i(t + \Delta t) = v\Delta t$. Moreover, there is a special point $\phi = \phi_c$ inside the cycle. The phase interval $0 < \phi_i < \phi_c$ corresponds to the evolution of the enzyme−substrate complex, while inside the interval $\phi_c < \phi_i < 1$ the product molecule is separated from the enzyme and the enzyme gradually returns to its free state. Since we assume that the product cannot bind back to the enzyme, forming again a substrate−enzyme complex, the reverse motion through the point $\phi_i = \phi_c$ should be forbidden in our algorithm. Thus, if the phase ϕ_i has already crossed the point ϕ_c and at a later time moment $t + \Delta t$ the phase given by eq 34 is less than ϕ_c, we replace it by $\phi_i(t + \Delta t) = \phi_c + v\Delta t$. Note that the phases vary in the interval (0, 1), and therefore the cycle described by eq 34 is terminated if we find that at the next time moment $\phi_i(t + \Delta t) > 1$.

The updating algorithms for the binary state variables s_i and r_i are

$$r_i(t+\Delta t) = \begin{cases} 1, \text{ if } r_i(t) = 0, \text{ with probability } \mu_i \Delta t \\ 0, \text{ if } r_i(t) = 0, \text{ with probability } 1 - \mu_i \Delta t \\ 0, \text{ if } r_i(t) = 1, \text{ with probability } \kappa \Delta t \\ 1, \text{ if } r_i(t) = 1, \text{ with probability } 1 - \kappa \Delta t \end{cases} \quad (35)$$

and

$$s_i(t+\Delta t) = \begin{cases} 1, \text{ if } s_i(t) = 0, \text{ with probability } \alpha_i \Delta t \\ 0, \text{ if } s_i(t) = 0, \text{ with probability } 1 - \alpha_i \Delta t \\ 0, \text{ if } s_i(t) = 1, \text{ and } \phi_i(t) = 1 \\ 1, \text{ if } s_i(t) = 1, \text{ and } \phi_i(t) < 1 \end{cases} \quad (36)$$

where the substrate binding rate is $\alpha_i = \alpha_0$ if $r_i = 0$ and $\alpha_i = \alpha_0/\chi$ if $r_i = 1$. The probability rate μ_i for binding a regulatory product molecule is given by

$$\mu_i = m(t)\beta(s_i,\phi_i) \quad (37)$$

where $\beta(s_i, \phi_i)$ is the product binding rate constant for an enzyme in the state characterized by s_i and ϕ_i. In the simulations for the model, introduced in section 2, $\beta(s_i, \phi_i) = \beta$ if $s_i = 0$ and zero otherwise. In the first modification in section 5 we have $\beta(s_i, \phi_i) = \beta$ independently on s_i and ϕ_i. In the second modification in section 5 we have $\beta(s_i, \phi_i) = \beta$ if $s_i = 0$ or $s_i = 1$ and $\phi_i < \phi_c$. The number m of product molecules is updated according to the stochastic algorithm

$$m(t+\Delta t) = m(t) + \sum_{i=1}^{N} \Theta(\phi_i(t) - \phi_c)\Theta(\phi_c - \phi_i(t - \Delta t)) - \sum_{j=1}^{m(t)} \zeta_j + \sum_{i=1}^{N} (r_i(t) - r_i(t + \Delta t)) \quad (38)$$

where ζ_j is a binary random number taking values 1 and 0 with probability $\gamma\Delta t$ and $1 - \gamma\Delta t$. The step function $\Theta(x)$ is defined as $\Theta(x) = 1$ if $x \geq 0$ and $\Theta(x) = 0$ if $x < 0$. The second term on the right side of eq 38 takes into account that a new product molecule is released and therefore m is increased by 1, whenever one of the enzymes goes through the phase point ϕ_c.

The third term describes the stochastic decay of products: each of m products can die with the small probability $\gamma\Delta t$ within time interval Δt thus decreasing the number m. The last term in this equation takes into account that the number m of free regulatory product molecules increases by 1 when a product molecule dissociates from an enzyme and decreases by 1 when a free product molecule binds to an enzyme.

The time step Δt should be chosen small enough, so that the conditions $\mu_i\Delta t \ll 1$, $\gamma\Delta t \ll 1$, $\kappa\Delta t \ll 1$, and $\alpha_i\Delta t \ll 1$ are fulfilled.

Acknowledgment. The authors acknowledge financial support from "Peter und Traudl Engelhorn Stiftung zur Förderung der Biotechnologie und Gentechnik" (Germany).

References and Notes

(1) Blumenfeld, L. A.; Tikhonov, A. N. *Biophysical Thermodynamics of Intracellular Processes*; Springer-Verlag: Berlin, 1994.
(2) Subbiah, S. *Protein Motions*; Springer: Berlin, 1996.
(3) Chen, E.; Goldbeck, R. A.; Kliger, D. S. *Annu. Rev. Biophys. Biomol. Struct.* **1997**, *26*, 327.
(4) Mozzarelli, A.; Rossi, G. L. *Annu. Rev. Biophys. Biomol. Struct.* **1996**, *25*, 343.
(5) Petsko, G. A. *Nature* **1994**, *371*, 740.
(6) Schlichting, I.; Berendzen, J.; Phillips, G. N.; Sweet, R. M. *Nature* **1994**, *371*, 808.
(7) Dickson, R. M.; Cubitt, A. B.; Tsien, R. Y.; Moerner, W. E. *Nature* **1997**, *388*, 355.
(8) Edman, L.; Mets, F.; Rigler, R. *Proc. Natl. Acad. Sci. U.S.A.* **1996**, *93*, 6710.
(9) Eigen, M.; Rigler, R. *Proc. Natl. Acad. Sci. U.S.A.* **1994**, *91*, 5740.
(10) Funatsu, T.; Harada, Y.; Tokunaga, M.; Saito K.; Yanagida, T. *Nature* **1995**, *374*, 555.
(11) Ishijima, A.; Kojima, H.; Funatsu, T.; Tokunaga, M.; Higuchi, H.; Tanaka, M.; Yanagida, T. *Cell* **1998**, *92*, 161.
(12) Lu, H. P.; Xie, X. S. *Nature* **1997**, *385*, 143.
(13) Chiu, D. T.; Clyde, F. W.; Ryttsen, F.; Strömberg, A.; Farre, C.; Karlsson, A.; Nordholm, S.; Gaggar, A.; Modi, B. P.; Moscho, A.; Garza-Lopez, R. A.; Orwar, O.; Zare, R. N. *Science* **1999**, *283*, 1892.
(14) Frauenfelder, H.; Sligar, S. G.; Wolynes, P. G. *Science* **1991**, *254*, 1588.
(15) Sfatos, C. D.; Shakhnovich, E. I. *Phys. Rep.* **1997**, *288*, 77.
(16) Socci, N. D.; Onuchic, J. N.; Wolynes, P. G. *J. Chem. Phys.* **1996**, *104*, 5860.
(17) Wang, J.; Onuchic, J.; Wolynes, P. G. *Phys. Rev. Lett.* **1996**, *76*, 4861.
(18) Gruler, H.; Müller-Enoch, D. *Eur. Biophys. J.* **1991**, *19*, 217.
(19) Häberle, W.; Gruler, H.; Dutkowski, Ph.; Müller-Enoch, D. *Z. Naturforsch.* **1990**, *45c*, 237.
(20) Schienbein M.; Gruler, H. *Phys. Rev. E* **1997**, *56*, 7116.
(21) Derenyi, I.; Astumian D. R. *Phys. Rev. L* **1998**, *80*, 4602.
(22) Hess, B.; Mikhailov, A. S. *Biophys. Chem.* **1996**, *58*, 365.
(23) Mikhailov, A. S.; Hess, B. *J. Phys. Chem.* **1996**, *100*, 19059.
(24) Stange, P.; Mikhailov, A. S.; Hess, B. *J. Phys. Chem.* **1998**, *102*, 6273.
(25) Hess, B.; Mikhailov, A. S. *Science* **1994**, *264*, 223.
(26) Hess, B.; Mikhailov, A. S. *J. Theor. Biol.* **1995**, *176*, 181.
(27) Hess, B.; Mikhailov, A. S. *Ber. Bunsen-Ges. Chem.* **1994**, *98*, 1198.